US 20030193333A1

(19) **United States**

(12) **Patent Application Publication** (10) **Pub. No.: US 2003/0193333 A1**

Barbic (43) **Pub. Date: Oct. 16, 2003**

(54) **SYSTEM AND METHOD OF MAGNETIC RESONANCE IMAGING**

(76) Inventor: **Mladen Barbic**, South Pasadena, CA (US)

Correspondence Address:
GREER, BURNS & CRAIN
300 S WACKER DR
25TH FLOOR
CHICAGO, IL 60606 (US)

(21) Appl. No.: **10/411,769**

(22) Filed: **Apr. 11, 2003**

Related U.S. Application Data

(60) Provisional application No. 60/372,003, filed on Apr. 12, 2002.

Publication Classification

(51) **Int. Cl.**[7] **G01V 3/00**

(52) **U.S. Cl.** **324/300**; 324/321; 324/307; 324/309

(57) **ABSTRACT**

A method of imaging a sample. A magnetic particle is positioned near a sample to be imaged. A strong direct current (DC) magnetic field is applied in a non-perpendicular direction relative to the sample, and a relatively weaker radio frequency (RF) magnetic field is applied. A plurality of polarized magnetic spins of the sample is produced in a region near the magnetic particle, and resonance of the plurality of magnetic spins is detected. The detected plurality of magnetic spins can be used to provide an image of the sample.

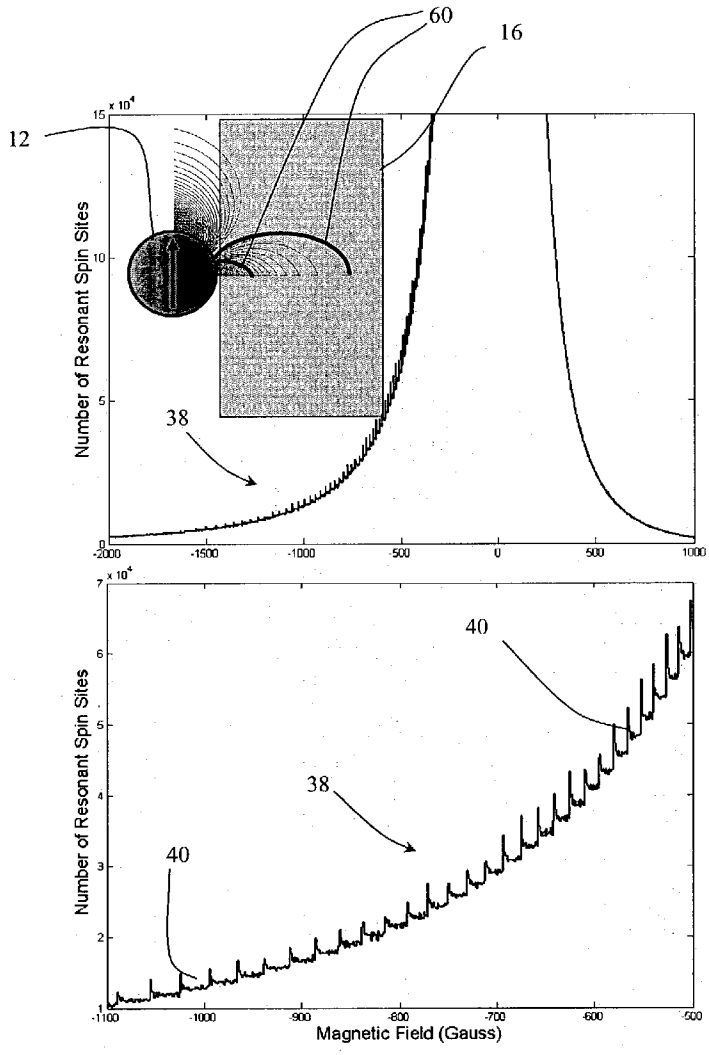

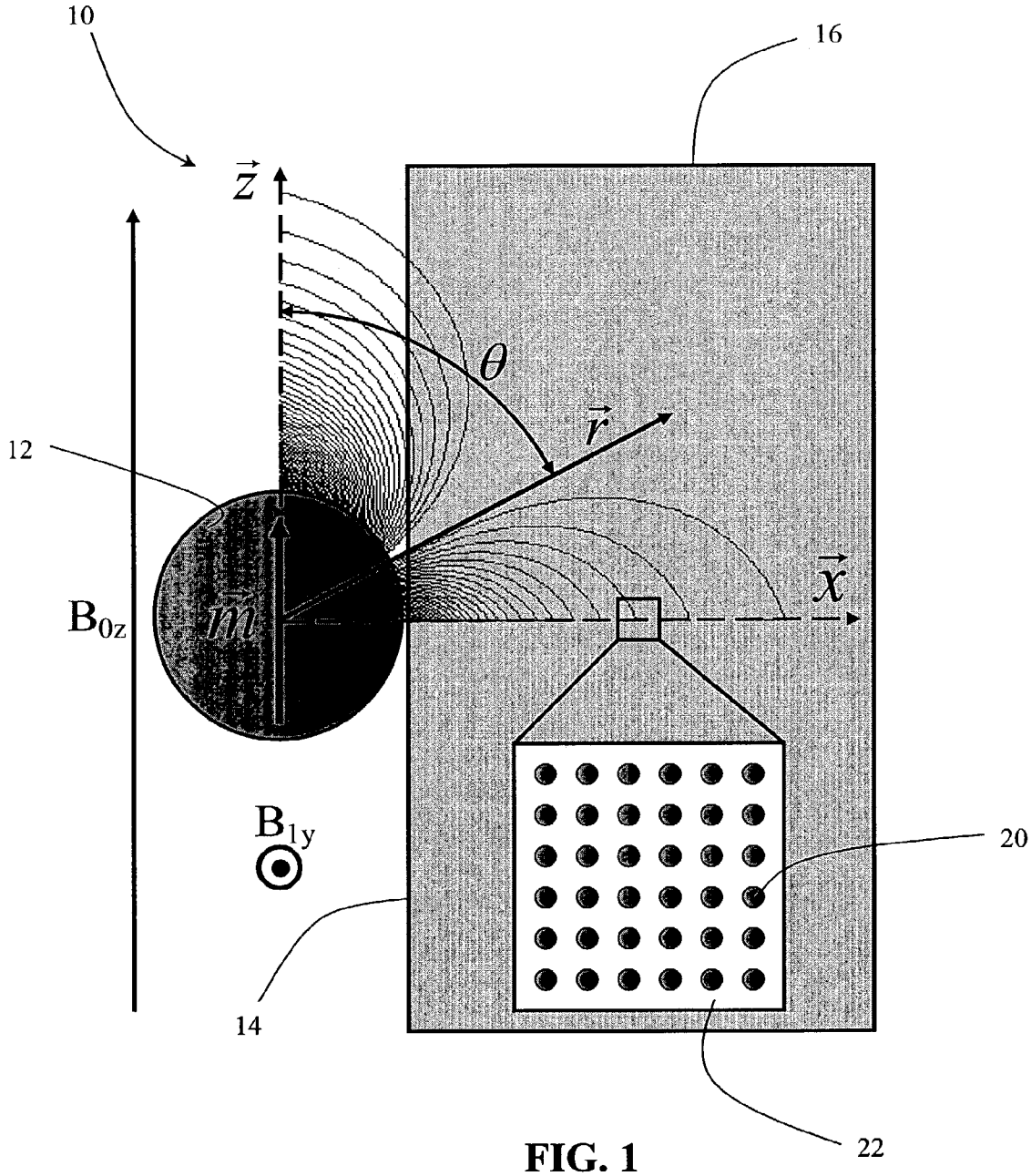

FIG. 1

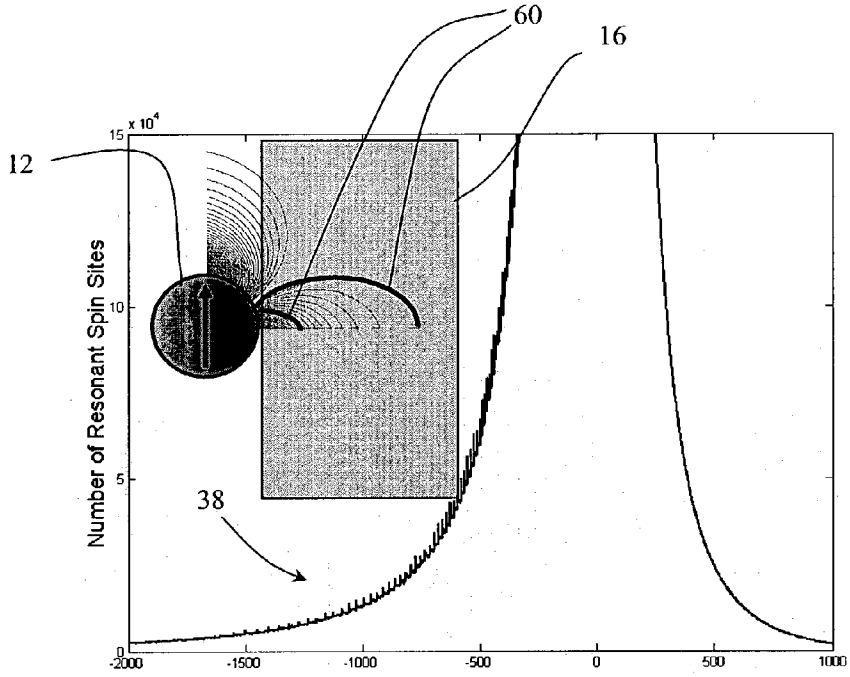
60
16
12
x 10^4
15
10
5
0
Number of Resonant Spin Sites
38
-2000
-1500
-1000
-500
0
500
1000

FIG. 2A

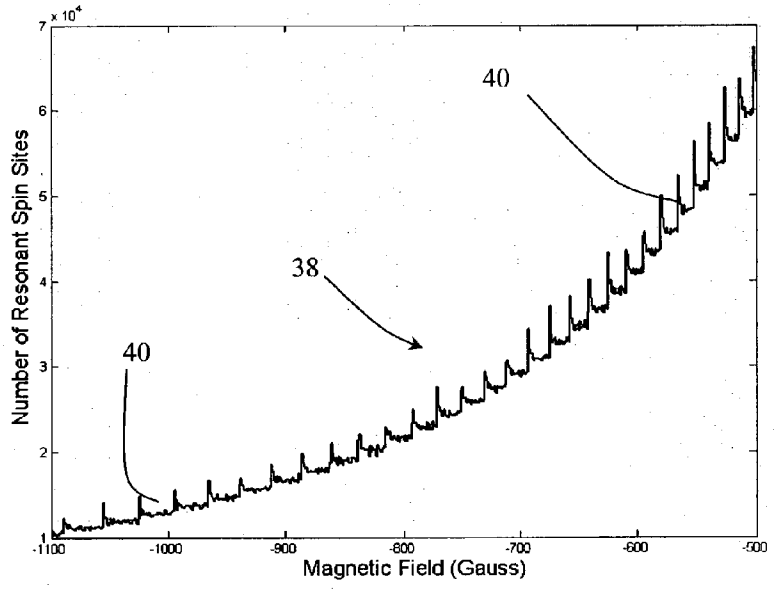
x 10^4
7
6
5
4
3
2
1
Number of Resonant Spin Sites
40
38
40
-1100
-1000
-900
-800
-700
-600
-500
Magnetic Field (Gauss)

FIG. 2B

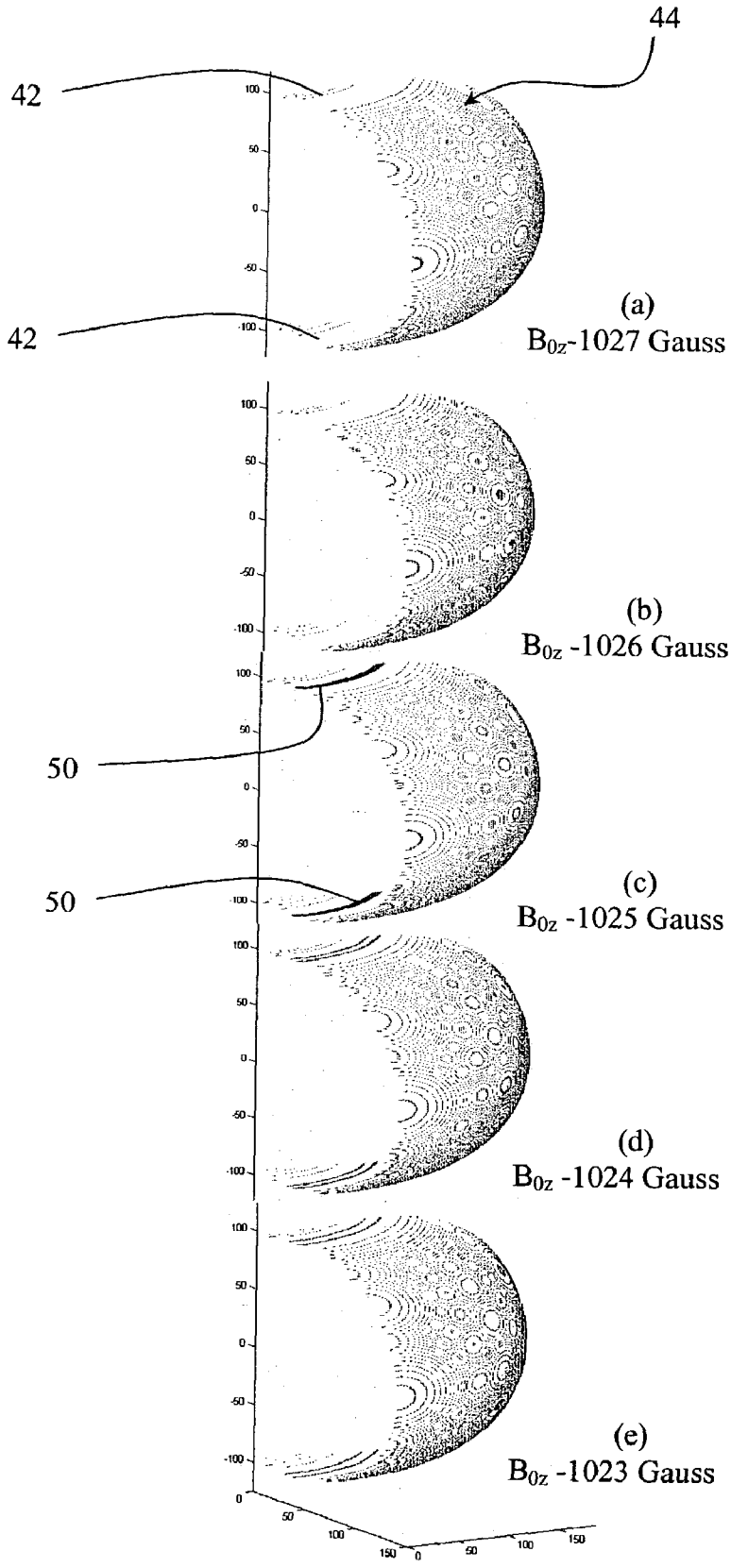
44
42
42
(a)
B_{0z}-1027 Gauss
(b)
B_{0z} -1026 Gauss
50
50
(c)
B_{0z} -1025 Gauss
(d)
B_{0z} -1024 Gauss
(e)
B_{0z} -1023 Gauss

FIG. 3

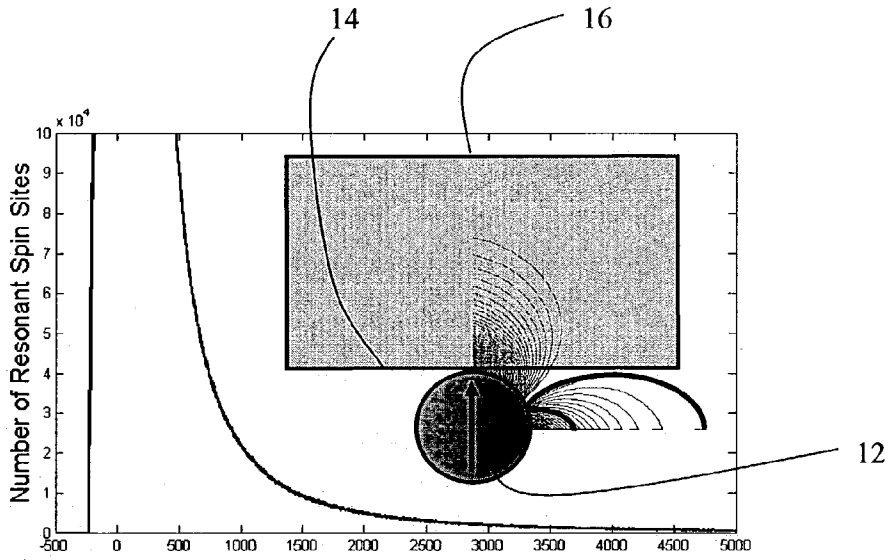

FIG. 4A

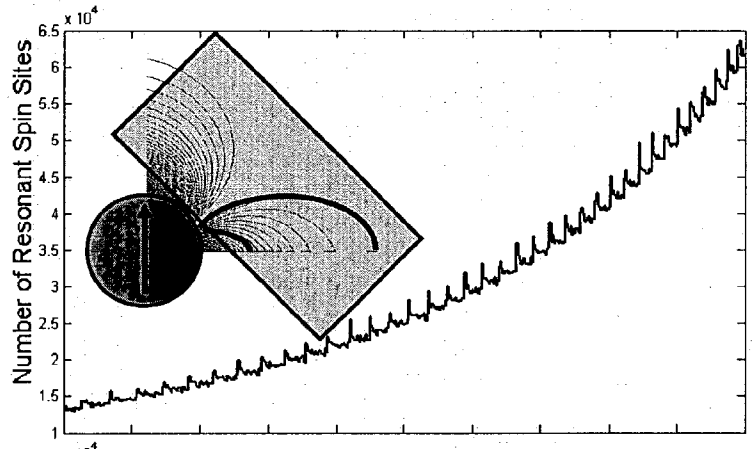

FIG. 4B

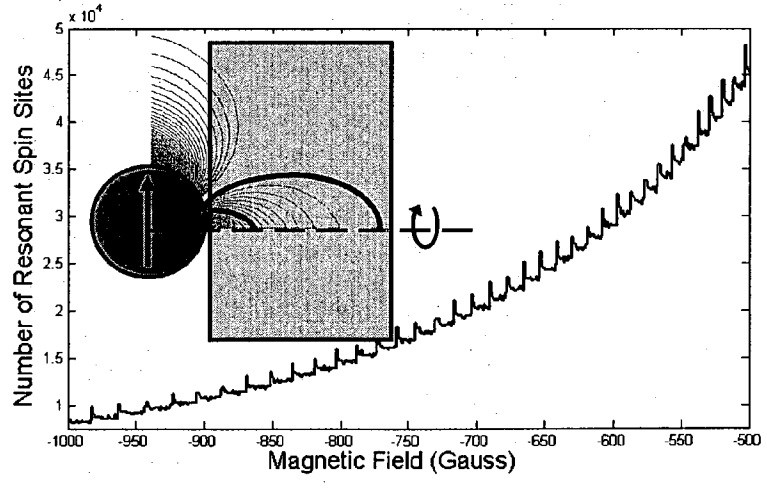

FIG. 4C

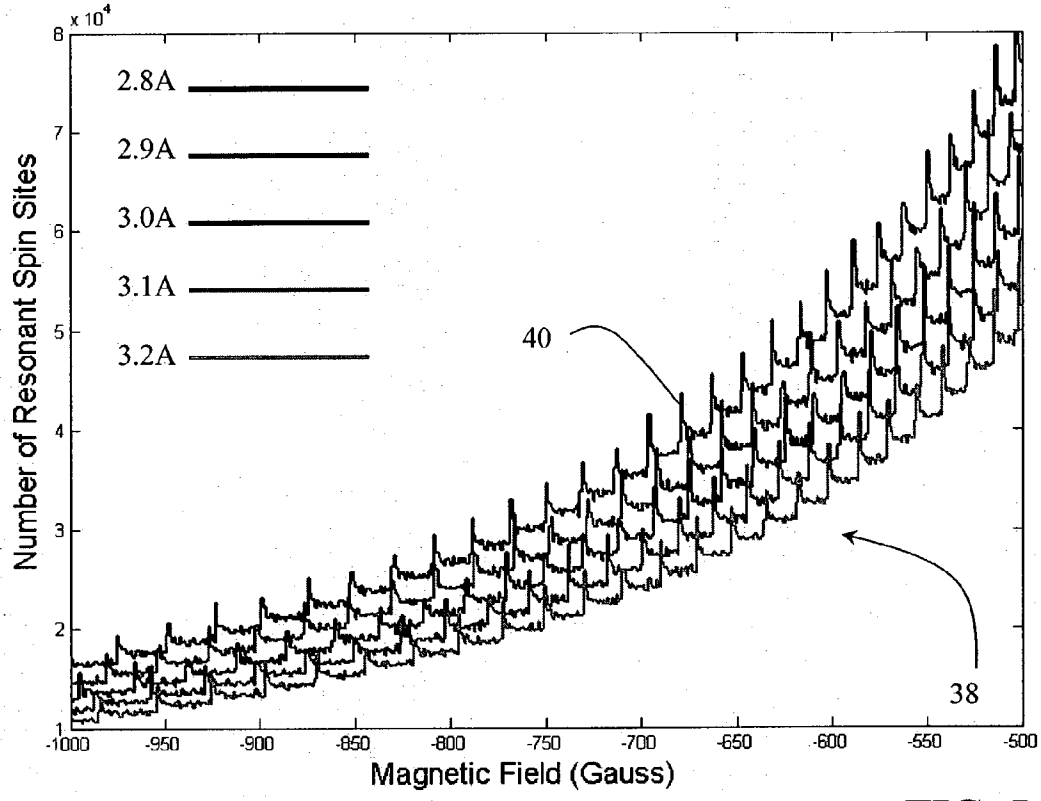
x 10^4
8
7
6
5
4
3
2
1
2.8A
2.9A
3.0A
3.1A
3.2A
40
38
Number of Resonant Spin Sites
-1000
-950
-900
-850
-800
-750
-700
-650
-600
-550
-500
Magnetic Field (Gauss)

FIG. 5

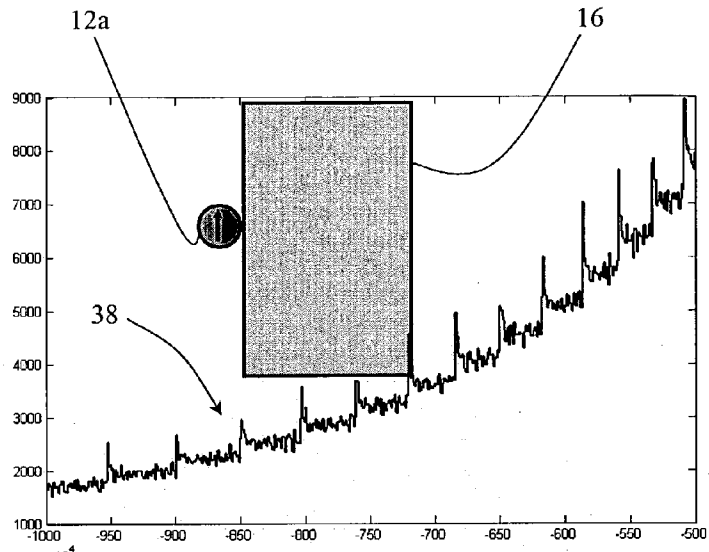

FIG. 6A

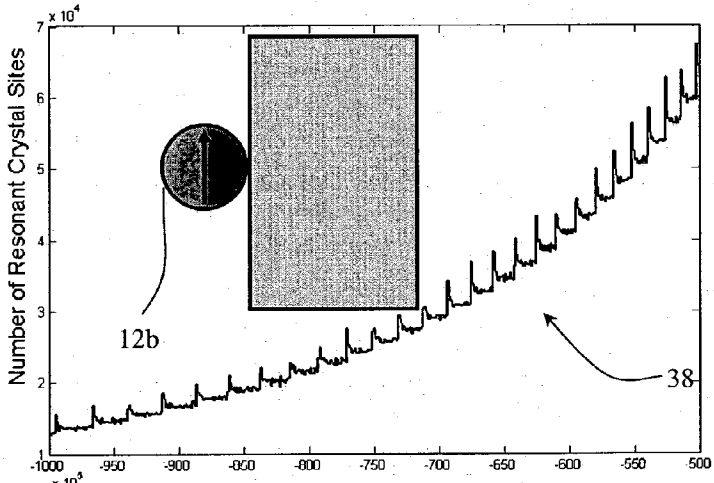

FIG. 6B

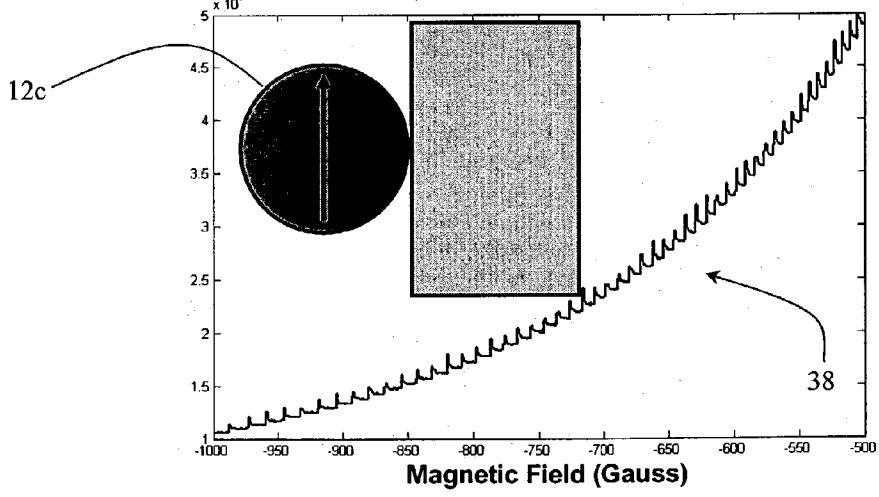

FIG. 6C

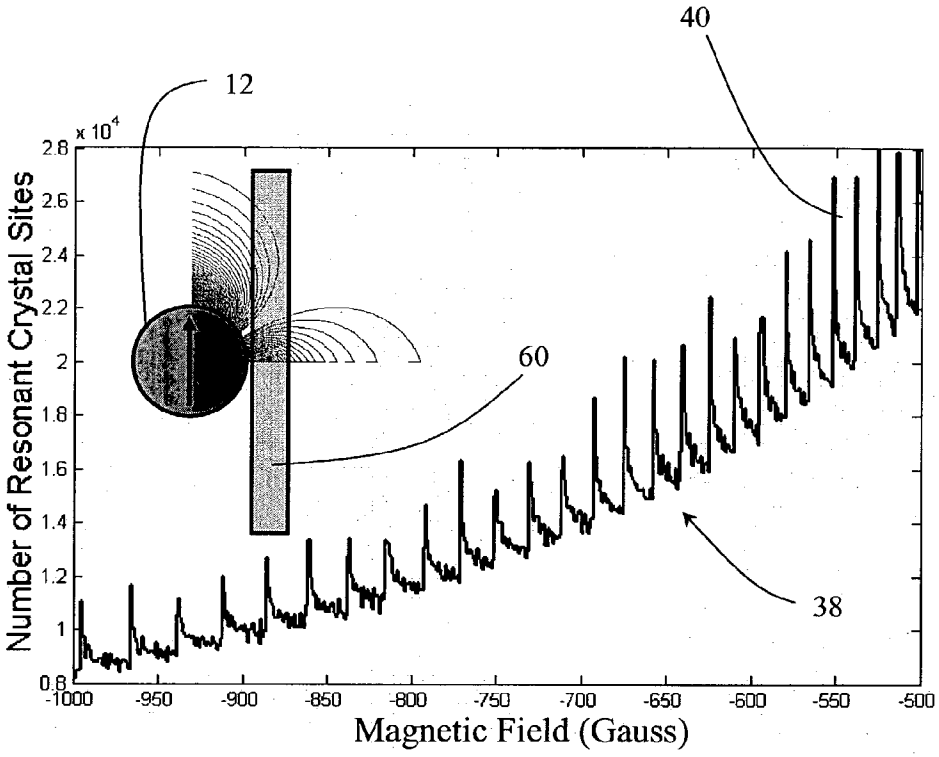
40
12
x 10^4
2.8
2.6
2.4
2.2
2
1.8
1.6
1.4
1.2
1
0.8
Number of Resonant Crystal Sites
60
38
-1000
-950
-900
-850
-800
-750
-700
-650
-600
-550
-500
Magnetic Field (Gauss)

FIG. 7

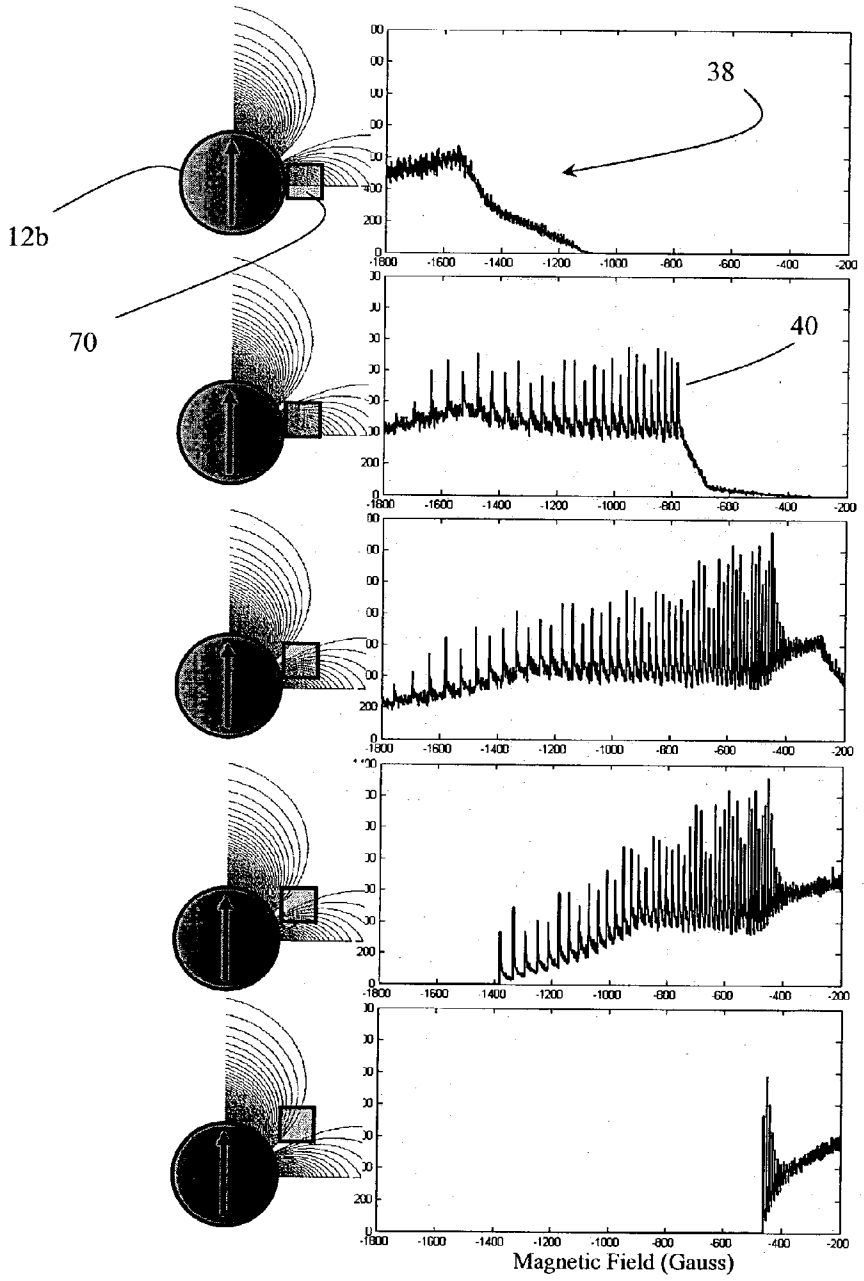

FIG. 8A

FIG. 8B

FIG. 8C

FIG. 8D

FIG. 8E

SYSTEM AND METHOD OF MAGNETIC RESONANCE IMAGING

PRIORITY CLAIM

[0001] This application claims priority of U.S. Provisional Patent Application Serial No. 60/372,003, filed Apr. 12, 2002, under 35 U.S.C. § 119.

STATEMENT OF GOVERNMENT INTEREST

[0002] This invention was made with Government assistance under National Science Foundation Grant No. NSF-DMR 97-24535. The Government has certain rights in this invention.

FIELD OF THE INVENTION

[0003] The present invention relates generally to the field of magnetic resonance imaging.

BACKGROUND OF THE INVENTION

[0004] Conventional magnetic resonance imaging has spatial imaging resolution of about 1 μm. Motivated by the potential of combining 3D imaging capability of conventional magnetic resonance and the atomic resolution of scanning probe techniques that utilize mechanical cantilevers, a new atomic resolution 3D magnetic resonance imaging technique was introduced. This method, magnetic resonance force microscopy (MRFM), uses a microscopic magnetic particle as a source of atomic scale imaging gradient fields and a mechanical resonator as a sensitive detector of magnetic resonance, as opposed to more conventional inductive techniques. Proof-of-concept demonstrations of MRFM were carried out for various magnetic resonance systems including electron spin resonance, nuclear magnetic resonance, and ferromagnetic resonance.

[0005] However, while MRFM is rapidly progressing by the incorporation of smaller magnetic particles and more sensitive mechanical resonators, current MRFM imaging resolution of ~1 μm remains at the level of conventional MRI inductive detection. A single nuclear or electron spin has not been successfully detected yet due to significant technical challenges.

[0006] Additionally, while achieving single spin sensitivity and resolution in a 3D imaging technique is of great significance, the MRFM technique also places challenging demands on the technical requirements, such as operation at very low temperatures, miniaturization of mechanical cantilevers, and the integration of magnetic nanoparticles into resonating structures.

SUMMARY OF THE INVENTION

[0007] The present invention provides a method of imaging a sample. In a preferred embodiment of the method, a magnetic particle is positioned near a sample to be imaged. A strong direct current (DC) magnetic field is applied to polarize the sample, and a relatively weaker radio frequency (RF) magnetic field is applied. Preferably, the direct current (DC) magnetic field is applied in a non-perpendicular direction to a surface of the sample. The DC field and/or RF frequency may be tuned to obtain resonance of the sample.

[0008] A plurality of polarized magnetic spins of the sample is produced, and resonance of the plurality of magnetic spins in a region near the magnetic particle is detected. The detected plurality of magnetic spins can be used to provide an image of the sample.

BRIEF DESCRIPTION OF THE DRAWINGS

[0009] **FIG. 1** is a schematic view of a model configuration for magnetic resonance imaging according to a preferred method of the present invention;

[0010] **FIG. 2A** is a histogram of the number of resonant spin sites of a 3 Angstrom unit cell size simple cubic crystal in the presence of a 100 nm diameter Cobalt ferromagnetic sphere, with an inset showing a model configuration with enhanced contours of constant B_Z;

[0011] **FIG. 2B** is an enlarged view of a portion of the histogram of **FIG. 2A**;

[0012] **FIG. 3** is a set of three-dimensional visualization plots of simultaneously resonant spin sites of a crystal lattice, for DC magnetic field values (shells of constant B_Z) of B_{Z0}-1027, B_{Z0}-1026, B_{Z0}-1025, B_{Z0}-1024, and B_{Z0}-1023 Gauss, respectively;

[0013] FIGS. **4A-4C** shows magnetic resonance spectra for three different angle configurations, respectively, of a sample with respect to a magnetic moment of a magnetic particle, with insets modeling the relative positions of the sample and magnetic particle;

[0014] **FIG. 5** shows magnetic resonance spectra from a simple cubic crystal with different unit cell dimensions;

[0015] FIGS. **6A-6C** show magnetic resonance spectra from a simple cubic crystal and Cobalt sphere dimensions of 50 nm, 100 nm, and 200 nm, respectively;

[0016] **FIG. 7** shows magnetic resonance spectra from a thin simple crystal film; and

[0017] FIGS. **8A-8E** show magnetic resonance spectra from a 100×100×100 atoms crystallite with a simple cubic structure and 3 Angstroms cell size, where the crystallite is scanned under a 100 nm Cobalt ferromagnetic sphere in 12 nm steps.

DETAILED DESCRIPTION OF THE INVENTION

[0018] The present invention provides a novel method of magnetic resonance imaging. According to the present method of imaging a sample, a magnetic resonance absorption signal is detected using the field from a magnetic particle. The absorption signal has features that are the direct signature of the atomic structure of the sample. Because different sample crystal structures have different spectral features, the technique can be used to study the crystal structure, for example, and chemical environment of the sample by magnetic resonance at the atomic level. The technique can be used in imaging of, as non-limiting examples, large crystals, thin films, or small crystallites. Other, non-crystalline materials are contemplated for imaging, as well.

[0019] The present invention provides a method of imaging using magnetic resonance for imaging a sample in close proximity of a magnetic particle, such as a sphere. A preferred embodiment of the invention includes positioning a small magnetic particle in close vicinity of a sample

surface, and applying a large polarizing field and a small radio-frequency field in a specific configuration so that absorption spectra reveals the crystal structure of the sample of interest. More particularly, a magnetic resonance signal is produced due to the presence of the magnetic particle, having a spectrum (or spectra) with sharp spectral peaks dependent on specific magnetic particle and magnetic field configurations. The appearance of the peaks is a direct signature of discrete atomic sites in the crystal lattice. The detection of these peaks may be used for atomic scale magnetic resonance. The positions of the spectral peaks are sensitive to the unit cell size of the sample, thereby providing a method for determination of the basic parameters of the sample at the atomic scale. The magnetic resonance spectra are dependent on the particle size and the angle of the particle magnetization with respect to the sample surface.

[0020] Although the method detects many nuclear or electronic spins at the same time, the present magnetic resonance technique allows sharp spectral features to appear that are a direct signature of the atomic structure. This is a significant distinction from other magnetic resonance techniques that seek to detect single spins, since one can determine the crystal structure even by detecting magnetic resonance from thousands of nuclear or electronic spins.

[0021] Using a preferred embodiment of the present method, the technical challenges of detecting magnetic resonance are reduced, due to the larger signal that can be obtained from many spins, but one can still obtain a magnetic resonance signal that reveals the atomic structure. The present method differs from, for example, the conventional MRFM method currently pursued for achieving single spin sensitivity and resolution by, among other things, employing an approach that relaxes the sensitivity requirements vis-a-vis MRFM by allowing many spins to coherently contribute to the magnetic resonance signal while still providing atomic scale information.

[0022] The preferred imaging method of the present invention has potential applications to the studies of, as non-limiting examples, crystals, thin films, and crystallites. Potential measurement methods for the confirmation of this imaging theory are also disclosed.

[0023] Referring now to the drawings, **FIG. 1** shows the basic model configuration of an imaging device **10** embodying a preferred method of the present invention. A magnetic particle **12** is positioned in proximity, for example, between zero (contact) to on the order of hundreds of nanometers, of a surface **14** of a sample **16**, preferably positioned via a mechanical positioner, for example, but not necessarily, a support such as a cantilevered or other support (not shown). The sample **16** may be, for example, a simple cubic lattice crystal. The magnetic particle **12** may be a sphere or other shape, such as, but not limited to, a pyramidal tip, conical tip, elongated ellipsoid, etc., and may have a size between, for example, on the order of tens of nanometers to several microns. Materials for the magnetic particle **12** may include, as non-limiting examples, Cobalt, Nickel, and Iron. Those in the art will appreciate that many other materials may be used. The sample **16** may vary in size, for example, between small crystallites and semi-infinite crystals.

[0024] In the exemplary method shown in **FIG. 1**, the magnetic particle **12** is a sphere 100 nm in diameter and made of Cobalt with a magnetization per unit volume of 1500 emu/cm^3. The exemplary sample **16** is a crystal, and is assumed to have a unit cell size of a_0=3 Angstroms. A large (as a non-limiting example, between 1 and 20 Tesla, but any sufficient magnetic field to cause polarization) direct current (DC) magnetic field B_0 is applied in a first direction that is non-perpendicular (for example, as shown in **FIG. 1**, parallel) relative to the surface **14** of the sample **16**. The magnetic field B_0 polarizes spins **20** of the atomic lattice **22** (a portion shown in enlarged view in **FIG. 1**) of the sample **16** for magnetic resonance investigation, and saturates the magnetization of the magnetic sphere **12**. As shown in **FIG. 1**, and by convention, though not required, the magnetic field B_0 is assumed to be in the z-direction.

[0025] For magnetic resonance investigation, a radio frequency (RF) field B_1 having intensity significantly smaller than that of the DC magnetic field B_0, is applied in a second direction, preferably perpendicular to the large polarizing DC magnetic field. The DC magnetic field B_0 may be, as a non-limiting example, between 100 and 1 million times the intensity of the RF field B_1. In the example shown in **FIG. 1**, the RF field B_1 is applied in the y-direction. The RF field B_1 is a magnetic field that may be applied to the sample **16** by a suitable device such as an inductive coil (not shown), micro-stripline, or other suitable devices.

[0026] In the absence of the magnetic sphere **12**, the atomic spin sites in the sample **16** would experience the same externally applied field B_0 and therefore meet the magnetic resonance condition at the same magnetic resonance frequency ω_R. However, close to (i.e. in a region of) the magnetic particle, a large magnetic field gradient is present within the sample **16**, for example, within a range on the order of 0.001-1000 Gauss/Angstrom, and only certain spin sites of the lattice of the sample satisfy the correct magnetic resonance conditions at any given magnetic field and frequency and therefore contribute to the magnetic resonance signal.

[0027] The magnetic field from the magnetic sphere **12** at a point r in the sample **16** has the azimuthally symmetric dipolar form:

$$\vec{B}(\vec{r}) = \frac{3\vec{n}(\vec{m}\cdot\vec{n}) - \vec{m}}{|\vec{r}|^3} \quad (1)$$

[0028] where n is the unit vector that points from the center of the magnetic sphere **12** to the crystal site location, and m is the magnetic moment vector of the sphere. Since the external DC polarizing magnetic field B_0 is considered to be much larger than the field from the magnetic sphere **12**, for example by ~10 Tesla, only the z-component of the magnetic field B_0 is included in considering the resonant spins **20** of the atomic lattice **22** of the sample **16**:

$$B_Z(\vec{r}) = \frac{M_0}{|\vec{r}|^3}(3\cos^2\theta - 1) \quad (2)$$

[0029] where θ is the angle between the z-axis (shown in **FIG. 1**) and the distance vector r as shown by example in **FIG. 1**, and M_0 is the magnitude of the saturation magnetic

moment of the magnetic sphere **12**. The contours of constant field B_Z are also shown in **FIG. 1**, and they have the azimuthally symmetric form around the z-axis.

[**0030**] If the magnetic sphere **12** is sufficiently small that the magnetic fields vary strongly on the atomic scale, steps are taken to account for the discrete nature of the crystal lattice. Labeling the atomic sites with indices (m, n, l), and assuming a unit cell size with dimension a_0, the components in expression (2) take the form:

$$\cos^2\theta = \frac{z^2}{r^2} = \frac{z^2}{x^2+y^2+z^2} = \frac{(la_0)^2}{(ma_0)^2+(na_0)^2+(la_0)^2} = \frac{l^2}{m^2+n^2+l^2} \quad (3)$$

$$|\vec{r}|^3=(x^2+y^2+z^2)^{3/2}=[(ma_0)^2+(na_0)^2+(la_0)^2]^{3/2}=a_o{}^3(m^2+n^2+l^2)^{3/2} \quad (4)$$

[**0031**] Incorporating equations (3) and (4) into equation (2), a final expression is derived for the z-component of the magnetic field B_Z from a magnetic sphere **12** at the atomic site with index (m, n, l):

$$B_Z(m,n,l) = \frac{M_0(2l^2-m^2-n^2)}{a_0^3(m^2+n^2+l^2)^{5/2}} \quad (5)$$

$$m = \{167,168, \ldots, +\infty\}$$

$$n = \{-\infty, \ldots, -1,0,+1, \ldots, +\infty\}$$

$$l = \{-\infty, \ldots, -1,0,+1, \ldots, +\infty\}$$

[**0032**] In this example, the index range for the x-axis starts with the integer 167, since expression (5) was derived for the 50 nm radius magnetic sphere **12** (166.66 times the lattice parameter a_0=3 Angstroms) at the center of the coordinate system. Those in the art will appreciate that these values can vary as the size, shape, and/or magnetization of the magnetic particle **12** vary, or for the sample 16, as the unit cell size, angle, or crystal structure vary, for example.

[**0033**] A prediction is made from the model when numerical summation is computed for the histogram of the number of resonant spin sites within a thin 1-Gauss wide shell of constant B_Z, as shown in **FIG. 2A**. This value of the bin width is selected since the line width broadening in solids is of the order of 1 Gauss. The bin width can be varied, for example using pulse techniques, to increase the resolution. The DC field is tuned swept over a certain range, preferably while the RF frequency is held constant, and/or the DC field is held constant preferably while the RF frequency is tuned (swept) or pulsed, to produce the spectrum. In the field range of the DC magnetic field B_0, for example between approximately B_{0Z}-1800 Gauss to B_{0Z}-200 Gauss as shown in **FIG. 2A**, sharp peaks **40** occur in spectrum **38** (the histogram of the number of resonant spin sites), while there are no distinguishable features in the positive magnetic field range. A magnified view of the spectrum **38** region between B_{0Z}-1100 Gauss to B_{0Z}-500 Gauss is shown in **FIG. 2B**.

[**0034**] The present inventor has discovered that at certain values for the magnetic field B_0 there are significantly (as shown, approximately 10-20%, at least) more resonant spin sites than for the adjacent magnetic field values, i.e. field values greater than or less than the particular values where the peaks occur. The present inventor further concluded that the appearance of the sharp magnetic resonance spectral peaks **40** is the direct signature of the discrete atomic lattice sites of the sample **16**. The spectrum **38** represents the image of the crystal lattice planes for the z-direction. By contrast, magnetic resonance of a continuous medium would result in a monotonic spectrum on the positive and negative values of the magnetic field B_0.

[**0035**] A clear explanation for the appearance of the sharp magnetic resonance spectral peaks **40** emerges when one visualizes the resonant spins under the influence of the magnetic field from the exemplary magnetic sphere **12** in three dimensions. **FIG. 3** shows five representation plots for crystal lattice spin sites of the sample **16** that are in resonance at a sequence of five values for the magnetic field B_0. Only the positive values for the y-axis indices are plotted for clarity. The magnetic field bin size is 1 Gauss, and the sequence is centered at the magnetic field value of B_{0Z}-1025 Gauss (shell (c)) the location of one of the sharp resonant peaks **40** in the spectrum **38** of **FIG. 2**. At the two higher magnetic field values of B_{0Z}-1027 Gauss and B_{0Z}-1026 Gauss (shells (a) and (b), respectively), there are two empty regions **42** at top and bottom sections **44** of the 1-Gauss thin shell of constant B_Z where no atomic spin sites are intersected. The reason is that at these magnetic field values, the top and bottom sections of the shell of constant B_Z from the magnetic sphere **12** are between the two lattice planes of the sample **16**, and do not intersect the atomic layers. However, there are still many atoms of the crystal that satisfy the resonance condition, as shown in shells (a) and (b), and they form the background signal in the magnetic resonance spectra of **FIG. 2**.

[**0036**] At the field value of B_{0Z}-1025 Gauss (shell (c)) for the DC field B_0 the shell of constant B_Z intersects the crystal lattice of the sample **16**, so that a large number of spin sites from the two lattice planes at the top and bottom sections of the resonant shell satisfy the resonance condition. Two bands **50** of the resonant atoms from the lattice planes are clearly visible in **FIG. 3**, and these are the resonant rings that are responsible for the sharp peaks in the magnetic resonance spectrum. At the next lower values of the magnetic field, B_{0Z}-1024 Gauss and B_{0Z}-1023 Gauss (shells (d) and (e), respectively), the bands **50** of resonant spin sites from the lattice planes slowly disappear as the top and bottom sections of the resonant shell of constant B_Z move between the next two adjacent atomic lattice planes. The inset diagram shown in **FIG. 2A** indicates the resonant shells **60** of constant B_Z with the lowest and highest magnetic field value in the spectra where the spectrum peaks occur. The spin sites between these border shells of constant B_Z are probed in this method of magnetic resonance imaging.

[**0037**] Magnetic resonance imaging using the magnetic field from the magnetic particle **12** thus results in sharp peaks in the spectrum **38** that reveal the underlying atomic structure. As opposed to using linear magnetic field gradients in resolving the crystal planes as in certain other methods, the magnetic particle **12** provides highly nonlinear magnetic field gradients. Nevertheless, as **FIG. 3** shows, the shells of constant B_Z intersect the crystal **16** in a way that allows one to resolve and reveal the underlying atomic lattice planes in the magnetic resonance signal. For the exemplary case shown in **FIG. 3**, the shells of constant B_Z intersect the <100> planes of the crystal **16** to give the

spectral peaks. This intersection of the shells of constant B_Z from the magnetic particle **12** through the crystal lattice draws an analogy to the Ewald construction in crystallography. However, in magnetic resonance imaging using the magnetic particle **12**, the intersection of the shells of constant B_Z occurs in the real space lattice, while the Ewald construction is carried out in the reciprocal lattice space.

[**0038**] Reasons for the appearance of magnetic resonance peaks of **FIG. 2** in the configuration of **FIG. 1** also reveal why such peaks were not predicted or observed in, for example, conventional MRFM investigations. The samples **16** in conventional MRFM work are normally positioned so that the magnetic moment m of the magnetic particle **12** is perpendicular to the sample surface **14**. This conventional configuration is shown in the inset of **FIG. 4A**. This choice of experimental conditions is made conventionally because the magnetic field gradient along the z-axis in such a configuration is twice as large as the gradient along the x-axis in the configuration of **FIG. 1**. However, by considering the intersections of shells of constant B_Z and the crystal lattice that result in the sharp spectral peaks, as shown in the inset of **FIG. 2A**, one realizes that none of the shells can intersect the crystal **16** in a way that would resolve and reveal the underlying atomic lattice planes. The graph shown in **FIG. 4A**, for example, shows the simulation for the configuration shown in the inset of **FIG. 4A**, where no clear, or sharp, signatures of the atomic lattices are present.

[**0039**] Although the peaks **40** are not evident for a crystal rotated at a **90** degree angle around the y-axis, as shown in **FIG. 4A**, much like in other crystallographic methods, the spectral peaks are expected at other angles where the thin azimuthally symmetric resonant shells of constant B_Z properly intersect the crystal lattice planes of the sample **16**. In the azimuthally symmetric system of **FIG. 1** there is no dependence of the spectra for crystal rotation around the z-axis. However, there is an angular dependence of the spectra on the rotation of the crystal **16** around the x-axis by the angle ϕ, as well as on the rotation of the crystal with respect to the y-axis by the angle θ. Two separate examples are given for the rotation of the crystal **16**: by 45 degrees around the y-axis in **FIG. 4B**; and by the same angle around the x-axis in **FIG. 4C**. As expected, the magnetic resonance spectral peaks **40** appear since the shells of constant B_Z properly intersect the atomic lattice planes of the crystal **16** at appropriate magnetic field values. Drawing on analogy with other crystallographic techniques, the shells of constant B_Z intersect the <110> and <101> planes of the crystal for the two cases shown in **FIGS. 4B and** 4C. The angular resolution of the sharpness of the spectral peaks **40** was also computed, and the linewidth of the angular resolution was found to be approximately Δ=0.5 degrees for the y-axis of rotation, and Δ=0.2 degrees for the x-axis of rotation.

[**0040**] The dependence of the spectral peaks **40** on the crystal lattice dimensions of the sample **16** and the magnetic particle **12** size and magnetization was also investigated. The spectra **38** for the five simple cubic crystal lattices with the unit cell size ranging from a_0 =2.8 Angstroms to a_0=3.2 Angstroms is shown in **FIG. 5**. There is a distinguishable difference among the five spectra **38** shown, with clearly different frequencies of the magnetic resonance peaks **40**. This feature is significant for potential crystallography applications, for example, since the different frequencies resulting from the method provide a measurement scale for distinguishing different crystal lattice dimensions.

[**0041**] As shown in FIGS. **6A-6C**, the variation in the size of the magnetic particle **12** (for the tests in FIGS. **6A-6C**, a sphere) also results in noticeable differences in the observed magnetic resonance spectra **38**. **FIGS. 6A, 6B**, and **6C** shows the spectra **38** for three different Cobalt spheres **12***a* **12***b*, **12***c* with diameters of 50 nm, 100 nm, and 200 nm, respectively. Observation of the spectra **38** reveals that the frequency of the magnetic resonance spectral peaks **40** is proportional to the diameter of the magnetic particle **12**, as is the number of resonant spins in each spectral peak **40**. This suggests an important trade-off, with smaller particles providing higher spectral (spatial) resolution, but with the requirement of higher sensitivity due to the smaller number of spins that needs to be detected. Larger magnetic particles provide lower spectral (spatial) resolution, but allow less stringent sensitivity requirements due to the higher number of spins that needs to be detected in each spectral peak **40**. Simulations of the effect of sphere moment m also reveal that higher moment materials for the particles **12** provide more numerous and sharper peaks at higher field values than lower moment particles. Therefore, Cobalt or Iron particles, for example, are preferred over lower saturation magnetization materials such as Nickel.

[**0042**] Further applications of the magnetic resonance imaging using, for example, particles **12** such as the magnetic spheres can be pursued with a closer analysis of the resonant spin sites within a thin shell of constant magnetic field B_Z, as shown in **FIG. 3**. It is apparent that the sharp spectral peaks **40** come from the very narrow regions of the sample **16**, while there is a large background signal from other resonant spin sites that are intersected by the 1-Gauss thick shell of constant B_Z. This feature of magnetic resonance imaging can be exploited in the studies of crystalline samples that are different from the semi-infinite crystal sample **16** of **FIG. 1**.

[**0043**] Referring now to **FIG. 7, a** simple cubic crystalline film **60** is shown in the inset, with a thickness of 100 unit cells in the x-direction but infinite in the y and z directions. The spectrum **38** expected from such a structure is shown in the graph of **FIG. 7**. The resonant peaks **40** occur at the same location as for the semi-infinite crystal sample **16** shown in **FIG. 1**, but they lack the large background signal because there are no atoms intersected by the resonant magnetic field shell beyond the 100th unit cell. This reduction in the large background signal would most certainly be advantageous in experimental work, and would qualify this magnetic resonance imaging technique for use in thin film studies. The same conclusions from the semi-infinite crystal sample **16** regarding the angular resolution and dependence of spectral peaks on the crystal unit cell size apply for the thin film crystal **60**.

[**0044**] In addition to the thin film crystalline structures **60**, the fact that only narrow sections of the sample **16** contribute to the peaks **40** in the magnetic resonance spectra could be applied to the studies of samples in the form of small crystallites. **FIG. 8** shows a simulation of a 100×100×100 atoms cubic lattice crystallite **70** scanned by the 100 nm diameter Cobalt magnetic sphere **12***b*. As the magnetic sphere **12***b* is scanned over the cubic lattice crystallite **70** in 12 nm increments, the spectrum **38** shows sharp resonant

peaks **40** in the narrow scan range of approximately 50 nm where the atomic lattice planes of the crystallite pass through the resonant slices of constant B_Z. A sequence of spectra **38** shows, as in the case of the thin film sample **60**, that the large background signal is almost non-existent in the magnetic resonance spectra. Therefore, even small crystallites would provide sharp peaks **40** in magnetic resonance spectra **38** with many spins in the atomic lattice planes coherently contributing to the signal.

[**0045**] As previously described, the new magnetic resonance imaging method disclosed provides an opportunity to detect the presence of atomic lattice planes by detecting the numerous spins that are coherently in resonance at the same value of the magnetic field. As a result, the preferred method potentially significantly relaxes the experimental constraints on the measurement from the single spin detection proposals of MRFM, for example, since a larger detected signal is available from additional spins. The present method also potentially alleviates potential single spin detection complications. Furthermore, the size of the magnetic particle **12** that would provide sufficient spectral resolution can be, for example, an order of magnitude larger than that believed to be necessary for single spin detection, further easing experimental realization of the technique. The number of spins that have to be detected in magnetic resonance imaging using the magnetic particle **12** may, for example, range between 10^4 and 10^5, and the number of spins in a spectral peak **40** above the background level is on the order of 10^3, as shown in **FIG. 2**. With the current sub-attonewton force detection capability using an ultra-thin cantilever and sensitive fiber optic interferometer, as well as the availability of the ultra-high magnetic field gradient sources, the detection of magnetic resonance imaging of spins using, for example, the magnetic particle **12** mounted on a mechanical cantilever is enabled. Although Cobalt is one preferred material, other materials with similar saturation magnetization but higher anisotropy such as, but not limited to, rare earth alloy PrFeB may be used, for example, to reduce thermal fluctuations.

[**0046**] Additionally, although the exemplary methods described herein may use a method similar to MRFM for the realization of magnetic resonance imaging, many other detection systems may be potentially used as well. These detection techniques may include, for example, micro-coil NMR, micro-SQUID detectors, Hall sensors, superconducting resonators, and microwave waveguides. These variations provide additional routes to the proposed atomic resolution magnetic resonance imaging.

[**0047**] Additionally, there are many other potential variations relating to the concept of magnetic resonance imaging using the magnetic field from the magnetic sphere **12**, including examining the magnetic resonance spectra **38** from crystal structures of samples **16** other than the simple cubic lattice described herein, and other potential experimental techniques for the sensitive detection of the magnetic resonance signal. Still further, although the methods disclosed herein has been described by example in the context of imaging and crystallographic applications, certain parallels between this imaging technique and other scientific topics where the interaction of the microscopic magnetic objects and discrete spins of the crystal lattice suggest other possible contexts, for example quantum computation.

[**0048**] While various embodiments of the present invention have been shown and described, it should be understood that other modifications, substitutions, and alternatives are apparent to one of ordinary skill in the art. Such modifications, substitutions, and alternatives can be made without departing from the spirit and scope of the invention, which should be determined from the appended claims.

[**0049**] Various features of the invention are set forth in the appended claims.

What is claimed is:

1. A method of imaging a sample, the method comprising the steps of:

positioning a magnetic particle near a surface of the sample;

applying a strong direct current (DC) magnetic field in a first, non-perpendicular direction relative to the surface of the sample;

applying a RF field in a second direction to produce magnetic resonance of a plurality of magnetic spins of the sample in a region near the magnetic particle;

detecting the magnetic resonance of the plurality of magnetic spins.

2. The method of claim 1 wherein said step of applying at least one strong direct current (DC) magnetic field comprises at least one of sweeping a strong direct current (DC) magnetic field wherein a frequency of the RF field is held constant, and sweeping the RF frequency wherein the DC magnetic field is held constant.

3. The method of claim 1 wherein the second direction is perpendicular to the first direction.

4. The method of claim 1 wherein the detected plurality of magnetic spins together form absorption spectra.

5. The method of claim 4 wherein the absorption spectra comprise a plurality of spin counts.

6. The method of claim 5 wherein each of the spin counts is for a different RF magnetic field frequency.

7. The method of claim 5 wherein each of the spin counts is for a different strong direct current (DC) magnetic field strength.

8. The method of claim 5 wherein the plurality of spin counts when aggregated produce a number of peaks.

9. The method of claim 8 wherein the peaks represent an atomic structure of the sample.

10. The method of claim 1 wherein said step of positioning comprises supporting the magnetic particle on a positioner and moving the positioner so that the magnetic particle is positioned near the sample.

11. The method of claim 10 wherein the magnetic particle is positioned against the sample.

12. The method of claim 1 wherein the magnetic particle comprises a magnetic sphere.

13. The method of claim 1 further comprising:

repositioning at least one of the magnetic particle and the sample in a scanning direction to a second position;

applying a strong direct current (DC) magnetic field in a first, non-perpendicular direction relative to the surface of the sample;

applying a RF field weaker than the strong magnetic field in a second direction to produce magnetic resonance of a second plurality of magnetic spins of the sample in a region of the magnetic particle;

detecting the resonance of the second plurality of magnetic spins.

14. The method of claim 13 wherein the plurality of magnetic spins and the second plurality of magnetic spins are used to produce an image.

15. The method of claim 1 wherein the sample is a crystal.

16. A method of imaging a sample, comprising:

positioning a magnetic particle near the sample;

applying a polarizing magnetic field to polarize the sample;

applying a RF field to cause a plurality of magnetic spins of the sample in a region to resonate near the magnetic particle;

detecting the resonance of the plurality of magnetic spins of the sample to produce absorption spectra, the absorption spectra including a plurality of peaks;

wherein the peaks are a signature of an atomic structure of the sample.

17. A method of measuring a sample, the method comprising the steps of:

positioning a microscopic particle near the sample;

applying a DC magnetic field to the sample;

applying an RF field to the sample;

detecting resonant spins at different values of at least one of the DC magnetic field and the RF field to produce spectra;

wherein the spectra provides a measurement scale for distinguishing crystal lattice dimensions of the sample.

* * * * *